Spatiotemporal intermittency in lines of vortices

H. Willaime, O. Cardoso, and P. Tabeling
Laboratoire de Physique Statistique, Ecole Normale Supérieure, 24, rue Lhomond, 75231 Paris, France
(Received 20 July 1992)

The turbulent regimes of lines of electromagnetically forced vortices are investigated experimentally. It is found that turbulence appears in the form of spatiotemporal intermittency. At lower values of the control parameter, a first regime is observed, characterized by spontaneous nucleation of the turbulent domains, and algebraic distributions of the lifetimes of the laminar domains. On the space-time diagrams, the bursts are associated with amplitude holes and rapid phase changes. At larger values of the control parameter the bursts connect and the system percolates. In this second regime, the distributions of the lifetimes of the laminar domains are exponential. The corresponding transitions appear to be of second order. A model of coupled oscillators, with coefficients measured experimentally, is shown to reproduce reasonably well the characteristics of the turbulent regime below the percolation threshold. In these experiments, percolation is found to be a useful concept for the description of turbulence, and the results suggest that nonadiabatic effects, such as the discrete nature of the system, play a role in the system.

PACS number(s): 47.27.Cn

I. INTRODUCTION

Spatiotemporal intermittency is a particular form of turbulence that consists of a space-time fluctuating mixture of coherent laminar domains and incoherent turbulent patches. This form of turbulence was first observed numerically [1] and later experimentally [2] in one-dimensional geometry. In the traditional view, a strong analogy is established between spatiotemporal intermittency and directed percolation [3]: according to this scheme, the turbulent patches appearing on the space-time diagrams are associated with active regions, the laminar ones with absorbing zones. Using such an analogy, and restricting ourselves to the simplest cases of directed percolation, we expect that the system undergoes a second-order phase transition from the laminar to the turbulent regime, with well-defined critical properties. Such a picture is in agreement with the results of a simulation of a modified Kuramoto-Shivashinsky equation, performed by Chaté and Manneville [1]. On the experimental side, it is also consistent with results obtained on convective systems [4] in rectangular and annular geometries, and more recently on the printer instability [2]. In all cases, the transition to turbulence has characteristics similar to a second-order phase transition. However, one also observes, in the same experiments, features which are difficult to reconcile with the traditional scheme, such as the spontaneous nucleation of the turbulent patches, the range of extension, in the control parameter space, of power-law distributions, and—for the printer instability—the existence of vectors of propagation of the turbulent domains. There have been some attempts to modify slightly the initial scheme in order to reproduce some of the observed phenomena [4]. Daviaud, Bonetti, and Dubois [4] assumed that, in addition to the directed percolation process, there is some small probability that turbulent domains nucleate spontaneously. This approach defines a problem depending on two parameters: one is related to the spontaneous nucleation, and the other one to the contamination. By working out a particular model of cellular automata, they could reproduce the imperfect nature of the transition observed in their experiment, and indeed the spontaneous nucleation of the bursts, although they did not find the same forms of histograms as in the experiment. Because of the presence of propagation vectors of turbulence, the experiments of Michalland and co-workers [2] apparently define another type of spatiotemporal intermittency. These results thus reveal a diversity of situations, which have in common the concepts of intermittency and percolation, but which do not exactly fit into the traditional scheme. A question that has been addressed recently is the origin of the turbulent patches, and their relation to the amplitude-equation formalism. A recent study of Daviaud *et al.* [5], performed on a system of coupled amplitude and phase equations, underlines the role of the Eckhaus instability in the nucleation of the bursts, which, at their early stage of formation, has a structure similar to Nozaki-Bekki holes [6]. Similar features have been obtained recently in the complex Ginsburg-Landau equation [6], so that one is tempted to consider that Nozaki-Bekki holes may play an important role, at least as precursor objects, in the spatiotemporal intermittent regimes.

In the present study, we investigate the form of weak turbulence arising in a quasi-one-dimensional flow—a linear array of forced vortices. In this system, we have previously characterized the ordered states, and observed interesting phenomena, such as frustration and short-wavelength instability [7]. It turns out that it is possible to reproduce its behavior by using a model of coupled oscillators forming a linear chain, for which the relevant parameters have been measured [8]. This system thus appears to be a good candidate to investigate one-

dimensional turbulence, for which only a few experimental studies have been carried out until now.

II. EXPERIMENTAL ARRANGEMENT

The experimental system that we use is represented in Fig. 1, and it is similar to that described in a recent paper [8]. The cell, made of plastic, is 40 mm wide and 50 mm high. Two lengths have been used (450 and 700 mm). In the top of the cell, a groove, 20 mm wide, of depth b, and covering almost the total length of the cell, is machined. For the various cells that have been made, b varies from 1.8 to 4 mm. In the bottom of the cell, there is a second groove, in which a line of alternated magnets, $5\times8\times3$ mm^3 in dimension, is formed. Each individual magnet produces a maximum magnetic field of 0.3 T. The resulting magnetic field, which is predominantly vertical, is close to a sinusoidal function of the coordinate directed along the magnet line, as shown in Fig. 2. Several lengths have been investigated, ranging from two up to 66 magnets. The cell is filled with a normal solution of sulfuric acid, at a level corresponding to the depth of the groove so as to suppress the meniscus along the boundary of the lattice; the surface of the fluid is free. We impose a steady electric current along the cell, and the resulting magnetic forces, which are spatially periodic, induce recirculating flows. We thus obtain a linear array of counter-rotating vortices, 8 mm wide and 20 mm long, whose number can be varied from one pair to 66 [as shown in Fig. 3(a)].

As shown in previous studies [9], as the electric current is increased, the system undergoes a transition from a state composed of counter-rotating vortices to a state where all the vortices have the same sign and are twice as large [see Fig. 3(b)]. This state will be further subject to temporal instabilities. We use the shadowgraph method [10] to visualize the separatrices between the vortices, and thus follow the spatiotemporal dynamics of the system (see Fig. 4, which represents the shadowgraph image of a system of 15 corotating vortices). For the measurements, the shadowgraph images are digitized, and the positions of the separatrices are determined by tracking, in real time, the maxima of the light intensity along the lattice axis. The resulting signal-to-noise ratio is about 40 dB.

From the signal obtained with the shadowgraph technique (see Fig. 4), we extract, for each separatrix, the instantaneous temporal phase and amplitude. For this, we register the position of each separatrix every half second. Every 8 s, we analyze the last 512 registered positions of the separatrices. The Fourier transform gives the spectrum of the signal. After filtering around the main frequency and keeping only the positive frequencies in the Fourier space, we perform the inverse Fourier transform. A mathematical analysis shows that the result is a complex function, the real part of which is the amplitude of the original signal and the imaginary part of which is the phase of this signal. To eliminate the windowing effect we only consider the "center" of the signal. So, we obtain the instantaneous value of the amplitude and the phase of the signal. This kind of method is already used in a similar context [6].

Another quantity that is determined from the shadowgraph image is the spatially averaged light intensity along the sides of the lattice. Such a quantity turns out to be very sensitive to the mean fluid level in the cell. The cell is thus connected to a reservoir, which is mounted on a

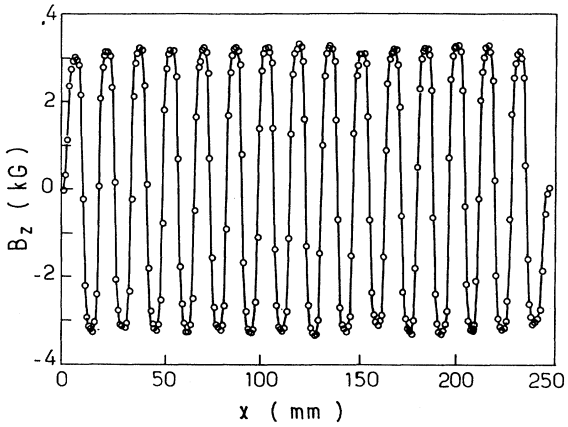

FIG. 2. Evolution of the vertical component B_z of the magnetic field, measured along the lattice axis x, just above the magnets, for a system of 30 elements.

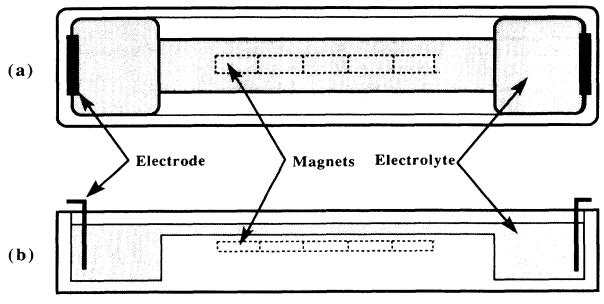

FIG. 1. Sketch of the experiment, with (a) and (b) the top and side views, respectively. The light gray region corresponds to the fluid, and the dark gray to the electrodes.

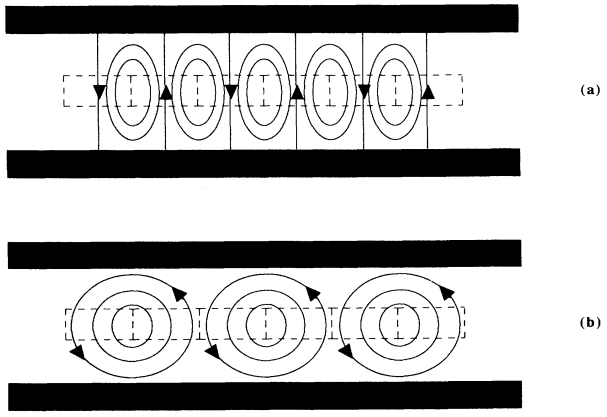

FIG. 3. Positions of the vortices in the cell. (a) shows the line of counter-rotating vortices, and (b) the corotating case.

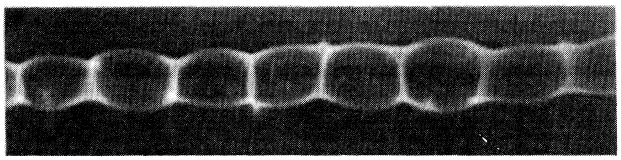

FIG. 4. Shadowgraph image of a system of 15 corotating vortices, produced by 30 magnets, with a fluid thickness of 3 mm.

stepping motor, and we monitor the motor so as to keep this quantity constant. By doing this, the fluid level can be held constant to within 0.5 μm, during periods up to 40 h.

III. RESULTS

A typical direct space-time diagram, close to the onset of the temporal instability, is shown in Fig. 5. Such a diagram represents the oscillations of eight separatrices in the central region of a lattice of 15 corotating vortices, for a fluid thickness of 3 mm. In this case, the electrical current is $I=14$ mA, and the temporal instability threshold is $I_c \approx 11$ mA. One has a monoperiodical regime, with a modulation of the amplitudes along the lattice. Phase measurements show that a wave, characterized by a wave number $k \approx 78°$ per unit of vortex, propagates along the lattice. Such a regime is typical of the ordered state. The existence of propagative waves at onset is related to the fact that the system behaves as a chain of coupled oscillators, with a negative value for the second-nearest-neighbor coupling [7]. One can therefore have "frustrated states," in the usual sense, i.e., coming from the competition between first- and second-nearest-neighbor couplings, and giving rise to propagative waves, in a way somewhat similar to helimagnetic systems. In our system, this effect is strong for $b=3$ mm, and is small, but still observable, for $b=2$ mm.

Figure 6 shows a typical space-time diagram at larger values of the current I. One can see the occurrence of intermittent bursts, which break the preceding order. Such

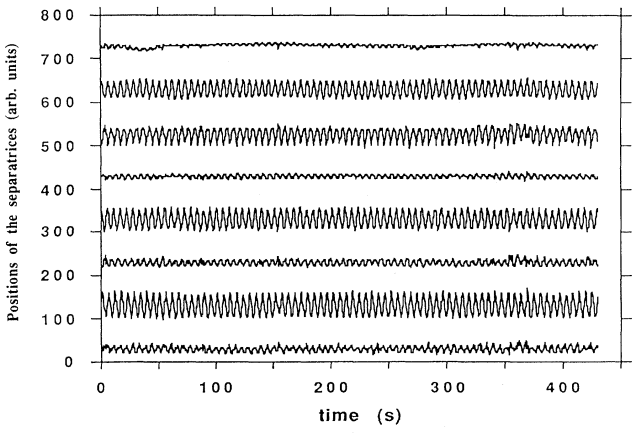

FIG. 5. Space-time diagram, for a system of eight separatrices, in the central region of a lattice of 15 corotating vortices, for $b=3$ mm, and $I=14$ mA.

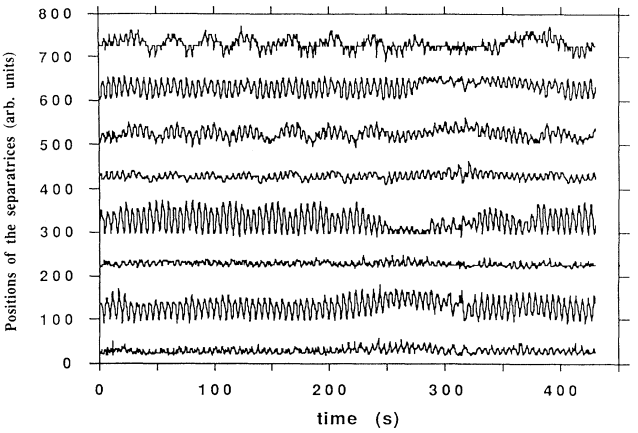

FIG. 6. Same as Fig. 5, but with $I=23$ mA, corresponding to the turbulent case.

events are random, have no well-defined characteristic duration, and are usually associated with a decrease in the amplitude of the signal. In order to characterize this regime, it is interesting to plot the amplitude $A(t)$ and the phase $\varphi(t)$ [actually the time derivative $\omega(t)=d\varphi/dt$ of the phase], as shown in Fig. 7. Bursts are clearly visible on the instantaneous frequency plot $\omega(t)$. The amplitude plot also shows that they are associated with amplitude holes. In our system, bursts correspond to rapid changes of the phase—and thus variations of the local wave number—together with the nucleation of amplitude holes.

One can represent, on a space-time diagram, the bursts, and perform some statistical measurements. In order to quantify the system, we use $\omega(t)$, and consider that the regime is turbulent when its deviation from the mean is larger than some threshold value. This condition amounts to imposing a condition on the local wave number. We further plot a space-time diagram similar to the one of Fig. 6, on which the bursts are represented by black regions, and the laminar zones by white regions. This is achieved in Fig. 8, which shows the evolution of such a diagram with the control parameter. One can see, as a general tendency, that the surface occupied by the bursts increases with the control parameter. Actually, two distinct situations arise: at lower values of I, the turbulent domains are localized, and they nucleate spontaneously. At larger values of I ($I>25$ mA), they tend to form a connected pattern and it becomes difficult to estimate the respective contribution of nucleation and contamination. On the basis of Fig. 8, there seems to be a percolation threshold in the system, located between 23 and 28 mA. This quantity is independent of the length of the system, as shown by experiments carried out with 66 magnets, and it seems to vary only slightly with the fluid thickness b (one finds typically 28 mA for $b=2$ mm).

Figure 9 shows typical histograms of the laminar domains below and above I_p. The quantity that is plotted in $N(\tau)$, i.e., the number of laminar domains of duration T that occur between τ and $\tau+d\tau$ (here $d\tau=2$ s). Well

below I_p, one obtains, in the lower range of values of τ, power laws for $N(\tau)$. The corresponding range typically extends from 10 to 100 s. Above this range, there is an exponential tail; for the lower range of values of τ, one obtains a power law in the form

$$N(\tau)=\tau^{-\nu} .$$

The value of ν is found independent of the length of the system; it depends slightly on the fluid thickness: one obtains $\nu\approx 1.7$ for $b=3$ mm and $\nu\approx 1.4$ for $b=2$ mm.

Well above I_p, the distribution $N(\tau)$ is exponential throughout the range of τ which is considered [see Fig. 8(b)], and the experimental data can be fitted by expressions in the form

$$N(\tau)=\exp(-\tau/\tau_0) ,$$

where τ_0 is a characteristic time. When I is close to I_p, one gets mixed distributions of $N(\tau)$, i.e., algebraic laws at small τ and long exponential tails at larger τ. Thus one can define in any case an exponent ν and a characteristic time τ_0.

In the context of the directed percolation transition, the laminar and turbulent regions correspond, respectively, to dry and wet zones (absorbing and active), and τ_0 can be viewed as the characteristic length of a nonwetted region, in the direction of the flow. Below the percolation threshold, τ_0 is infinite, and it is finite above it. It is thus of interest to represent the variations of τ_0^{-2} with I (see Fig. 10, obtained for $b=2$ mm). Below $I_p=21$ mA, one finds that τ_0^{-2} is small, and the corresponding values of τ_0 are several thousand periods of oscillation. This indicates that the system is below the percolation threshold. Above I_p, one finds a sudden decrease of τ_0 and its typical values are now several periods of oscillation; this indicates that we have crossed a percolation transition. I_p can thus be considered as the percolation threshold of the system, and the evolution of τ_0 is consistent with a second-order phase transition. Similar features have been observed for $b=3$ mm.

Another statistical measure of the turbulent regime is the turbulent fraction F_t, defined as the ratio of the surface occupied by the turbulent domains in the space-time diagram of Fig. 8 over the total surface. The variation of F_t with the control parameter is shown in Fig. 11 in the case $b=3$ mm. One obtains a continuous increase of F_t above the onset of the intermittent regime $I_t=21$ mA. A

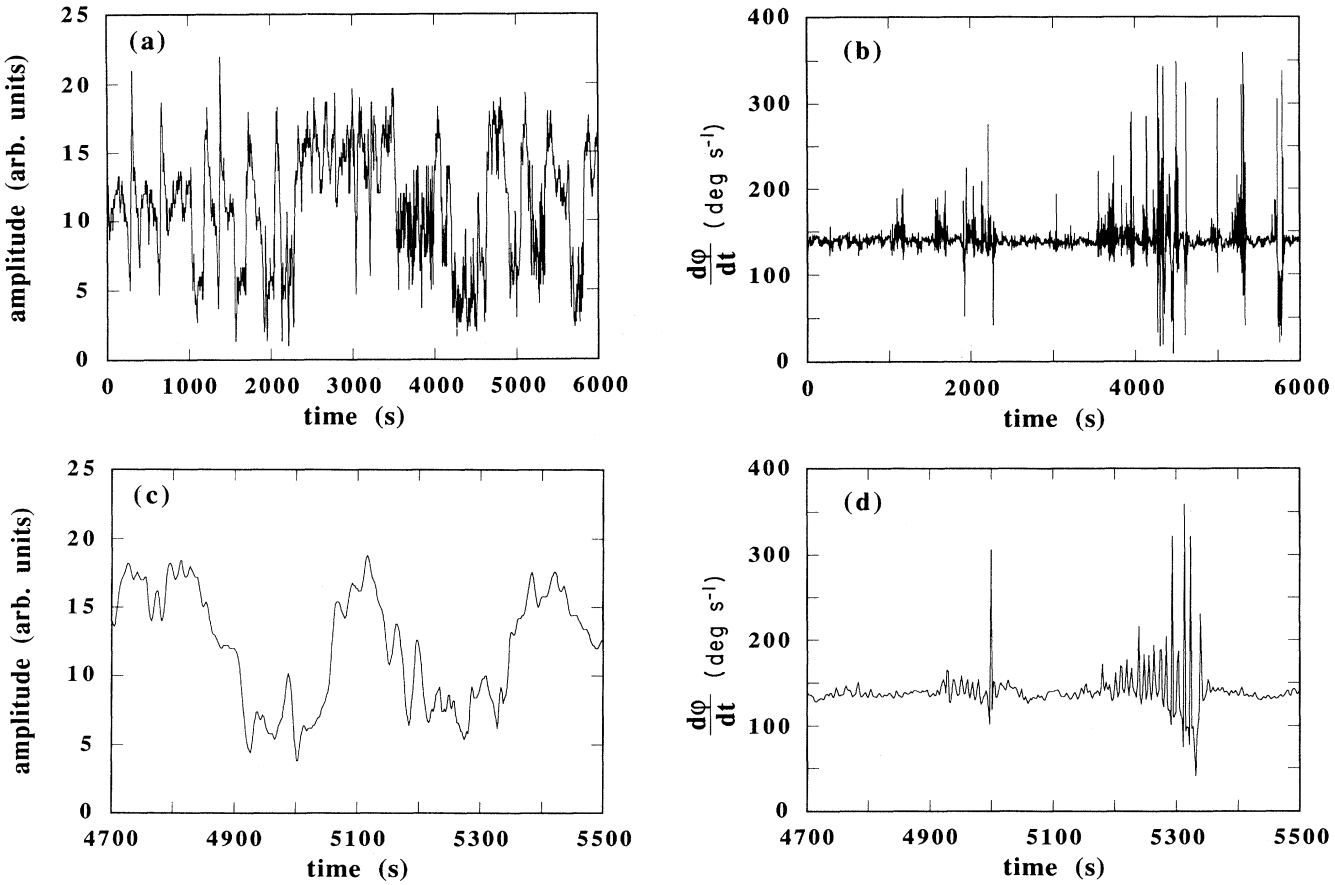

FIG. 7. Amplitude and phase of the fluctuations of the position of a single separatrix, in the turbulent regime, i.e., for $I=22$ mA, with $b=3$ mm. (a) and (b) are long-time recordings, while (c) and (d) correspond to a shorter period, so as to reveal the structure of the intermittent bursts.

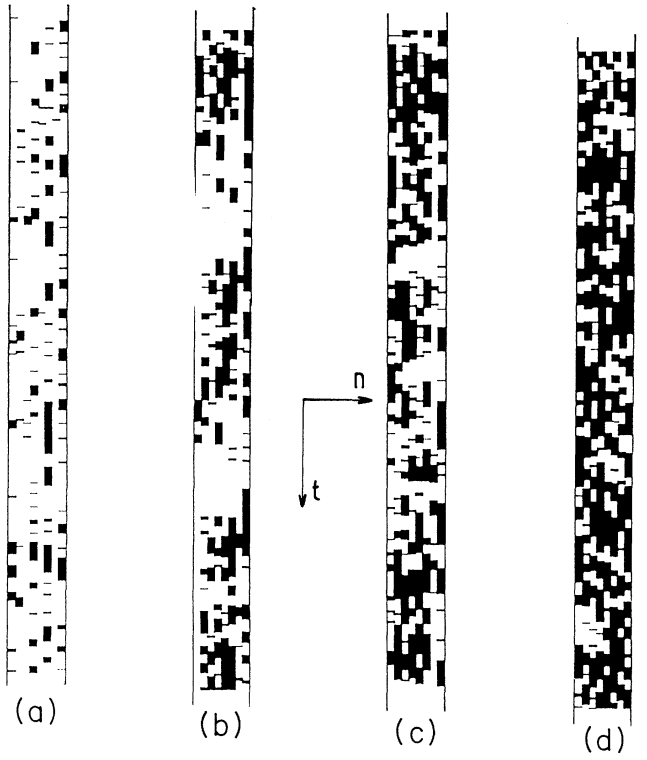

FIG. 8. Space-time diagrams, for different values of I, with $b=3$ mm, for which the turbulent bursts are represented by black regions. (a) $I=21.5$ mA; (b) $I=23$ mA; (c) $I=25$ mA; (d) $I=29.5$ mA.

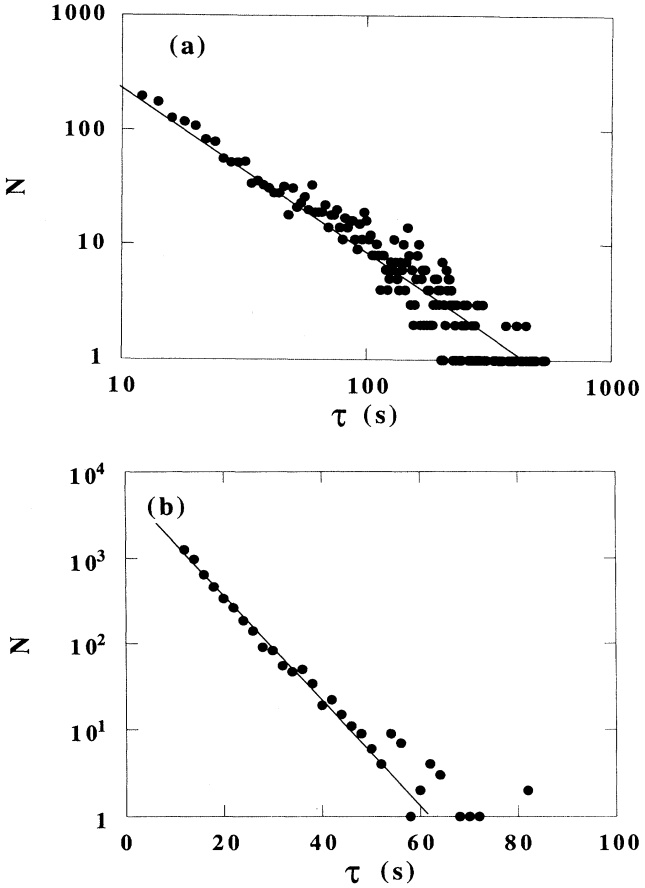

FIG. 9. Number $N(\tau)$ of laminar phases with duration between τ and $\tau+\delta\tau$, for $b=3$ mm, and different values of I. (a) $I=22.5$ mA; (b) $I=28$ mA.

reasonable fit of such a curve is given by the expression

$$F_t \sim (I-I_t)^{0.5} .$$

The system percolates as the turbulent fraction becomes larger than about 50%.

These results thus show the existence of two thresholds: the first one, at $I=I_t$, corresponds to the onset of turbulence, and the second one, located at $I=I_p>I_t$, defines a percolation transition. Above I_t, and below I_p, the dynamical regime is characterized by turbulent patches, localized both in space and time, and nucleating spontaneously. We shall call it regime A. As I is increased above I_t, the turbulent fraction increases and finally the system percolates at $I=I_p$. Above this threshold, the turbulent patches form a connected pattern, and the characteristic length of the laminar domains is finite. We shall call it regime B.

All the above features, which have been obtained with lattices of up to 16 corotating vortices, have also been observed on a longer cell, including 33 vortices.

IV. COMPARISON WITH A MODEL OF COUPLED OSCILLATORS

Due to the one-dimensional geometry and the fact that the vortices are produced by a forcing mechanism, it is tempting to compare our system to a chain of coupled oscillators [8]. In the model that we have proposed, the dynamic of each individual oscillator is characterized by a complex number $W_n(t)$, i.e., an amplitude and a phase; and, in agreement with the experiments performed on systems of small sizes, each of them results from a Hopf supercritical bifurcation. Concerning the interaction

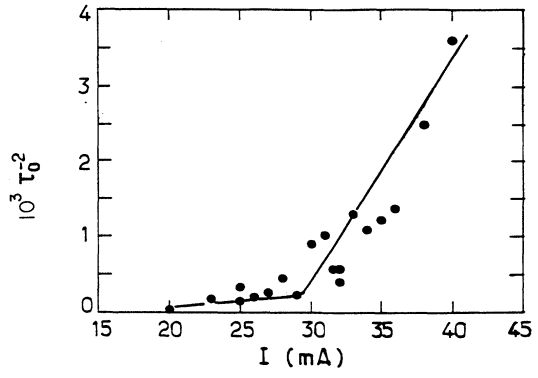

FIG. 10. Evolution of the characteristic time τ_0 with the control parameter I, for $b=2$ mm.

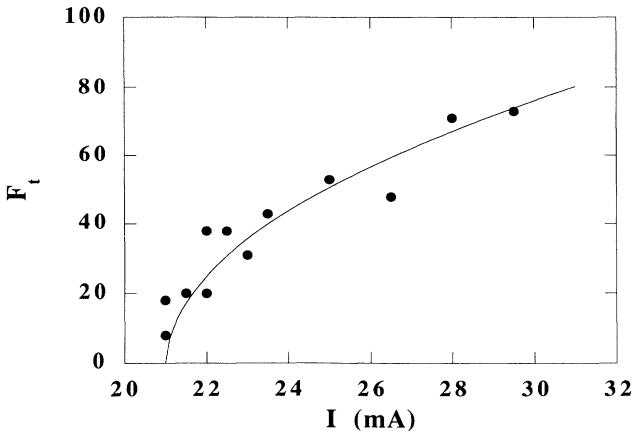

FIG. 11. Evolution of the turbulent fraction F_t with the control parameter I, for $b=3$ mm.

with the lattice, we introduce both linear and nonlinear, first- and second-nearest-neighbor couplings. One thus gets a dynamical system of N equations, which governs the evolution of the system, in the form

$$\frac{dW_n}{dt}=\mu(1+ic_0)W_n-(1+ic_2)W_n|W_n|^2 +\epsilon(1+ic_1)(W_{n-1}+W_{n+1}) -(c_3+ic_4)W_n(|W_{n-1}|^2+|W_{n+1}|^2) +\epsilon'(1+ic_1')(W_{n-2}+W_{n+2}) , \quad (1)$$

where $\mu=(I-I_c)/I_c$. Here, μ is the control parameter of the system, I_c is a threshold value, and c_0, c_1, c_2, c_3, c_4, c_1', ϵ, and ϵ' are real numbers. The linear modes of instability of the chain are traveling waves in the form $W_n=W_0e^{i(\omega t+kn)}$. When ϵ' is positive, the critical modes are either acoustical (for ϵ positive) or optical (for ϵ negative), as in the case $\epsilon'=0$. Frustrated states are obtained when ϵ' is negative, and is larger in absolute value than $\epsilon/4$. In this case, the linear modes of instability are traveling waves with wave number different from 0 and π.

We have measured the parameters of such a model, for the two cases $b=2$ and 3 mm. The values are given in Table I [7].

From Eq. (1), one can calculate the equation of the marginal stability curve. One finds

$$\mu=-2\epsilon\cos(k)-2\epsilon'\cos(2k) .$$

The corresponding curve is plotted in Fig. 12, in the case $b=3$ mm. The Eckhaus boundary and the limit of onset for short-wavelength instability have also been computed and the corresponding lines are represented in the same figure. In order to compare with the experiment, we have represented, on the same diagram, the evolution of the mean local wave number (obtained by measuring the phase difference between each pair of separatrices), as the control parameter $\mu=(I-I_c)/I_c$ is increased. One finds that spatiotemporal intermittency arises as the system penetrates into an Eckhaus instability band. This remark suggests that, in our system, the origin of the turbulent bursts is related to the Eckhaus instability.

The system (1) has been solved numerically for values of the control parameter for which we expect to find turbulence. Figure 13 shows the space-time diagram for $W_n(t)$, and Fig. 14 the evolution of the instantaneous frequency $\omega(t)$ and the amplitude $|W(t)|$ for a single oscillator, for $\mu=0.328$, $N=15$ (this corresponds to $I\approx 20$ mA in the 3-mm case). One finds intermittency, in agreement with the experiment; in both cases, the bursts, which are clearly visible on $\omega(t)$, are associated with amplitude holes. The corresponding space-time diagram, obtained with the same criterion as the experiment, is displayed in Fig. 15, for several values of μ. One finds a slow increase of the number of bursts with μ, but there is no evidence for the existence of a percolation transition. In every case, they nucleate spontaneously, but never form a connected pattern. For this regime, it is of interest to plot, as in the experiment, the distribution of the duration of the laminar domains (see Fig. 16). One finds a power law, in the form

$$N(\tau)=\tau^{-\nu} ,$$

where $\nu\approx 1.8$, which is close to the experimental value. This value is found independent of μ, in the limit where intermittency indeed exists. One thus recovers the algebraic experimental distribution. Contrary to the experi-

TABLE I. Values of the parameters in Eq. (1) in the cases $b=2$ and 3 mm.

	$b=2$ mm	$b=3$ mm
I_c	11 mA	15 mA
c_0	2.10	−0.11
c_1	−4.3	0.22
c_2	−0.20	−1.34
c_3	−0.08	3
c_4	−1.20	0.046
ϵ	−0.05	0.23
c_1'	neglected	0.22
ϵ'	−0.016	−0.23

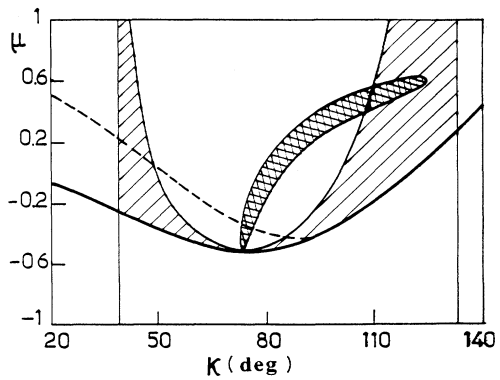

FIG. 12. Marginal stability diagram, obtained for the case $b=3$ mm, together with the Eckhaus band (hatched region), the boundary of short-wavelength instability (dashed line), and the region visited by the experiment (cross-hatched region).

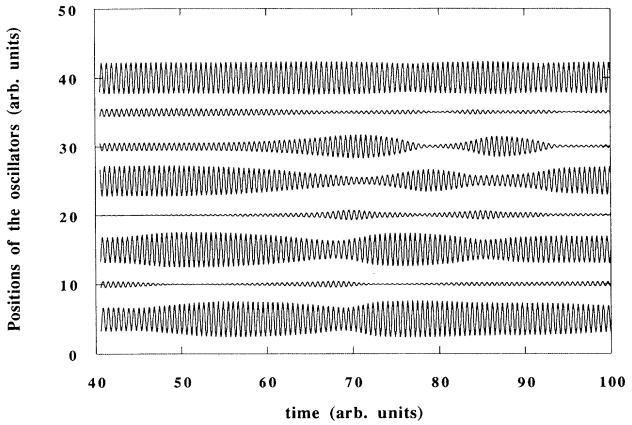

FIG. 13. Space-time diagrams, deduced from the model (1), for $\mu=0.328$.

ment, we do not find exponentially decreasing regimes for the distribution of τ. One can thus consider that the model reproduces correctly the form of turbulence, which is observed experimentally, close to the onset of intermittency and below the percolation threshold.

It is interesting to check if the discrete character of the model plays a role in the observed phenomena. In order to do that, we have applied directly, in the corresponding equations, the continuous limit $k \to 0$ and solved numerically the resulting complex Ginsburg-Landau equation. The result is that the system remains stable for any value of μ. If we impose initial conditions such that the system lies within the unstable Eckhaus band, one observes a transient state during which bursts, similar to those obtained in regime A, are nucleated at random. However,

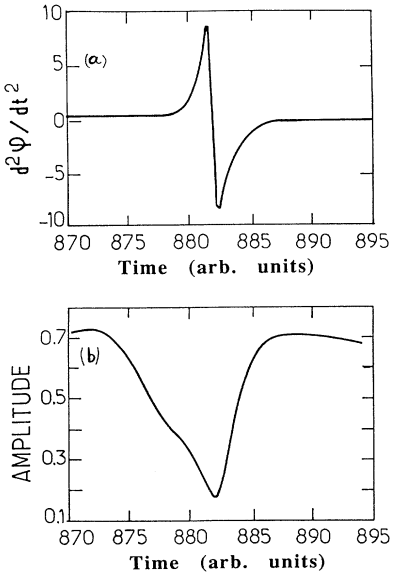

FIG. 14. Evolution of the amplitude and the phase derivative of $W(t)$, using (1), with $\mu=0.328$.

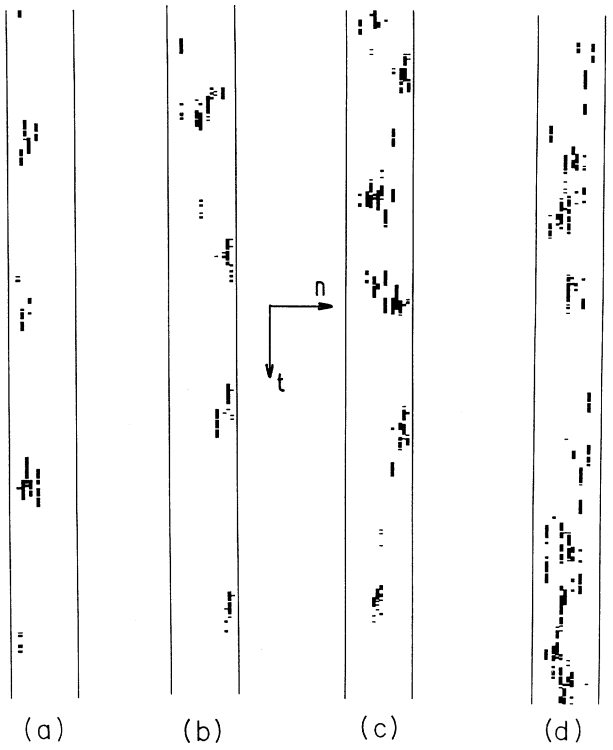

FIG. 15. Space-time diagrams, for $N=15$, different values of μ, and for which the turbulent bursts are represented by black regions. The axes (time t, index of the oscillator n) are shown; (a) $\mu=0.104$; (b) $\mu=0.192$; (c) $\mu=0.312$; (d) $\mu=0.344$.

the system quickly returns to an ordered stable state of oscillation. The role of the discretization is therefore essential to maintain the system in an unstable zone.

V. DISCUSSION

As mentioned in the Introduction, the standard view of spatiotemporal intermittency bears upon an analogy, suggested by Pomeau, between the transition to turbulence

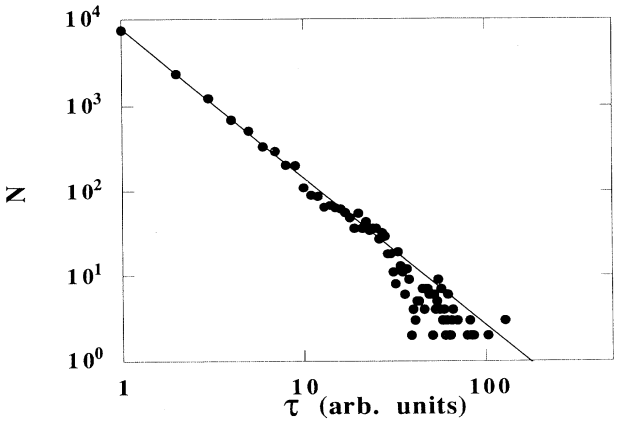

FIG. 16. Histogram of the laminar regions, for $\mu=0.344$, $N=15$.

and directed percolation. In this view, the turbulent domains nucleate by contamination, the transition to turbulence is of second order, and histograms of the duration of the laminar domains are exponential, except at the threshold where the form of the algebraic prefactor can eventually be revealed [3]. This view may be appropriate for our system above I_p, but it does not provide a description of the regime which we observe between I_t and I_p, i.e., regime A, because of the spontaneous nucleation of the turbulent patches and the forms of the histograms. Our system thus represents a situation where two nucleation processes are present (spontaneous nucleation and contamination), somewhat similar to convection experiments performed in annular geometry [4].

Concerning now the origin of the bursts and their structures, our results suggest that they are related to the Eckhaus instability. A similar remark was made by Daviaud *et al.* [5] in the context of a convection experiment. In our case, the structure of the bursts, even close to their onset, seems to be more complex than "ordinary" Nozaki-Bekki holes. In particular, the regions just outside the amplitude holes cannot be simply characterized by homogeneous wave numbers. Therefore, even if there is some analogy between the bursts that we observe and objects such as Nozaki-Bekki holes, one can hardly establish a strong connection.

Finally, the fact that the model of nonlinearly coupled oscillators reproduces the characteristics of regime A, both qualitatively and quantitatively, is notable. Compared to the Ginsburg-Landau equations, our model incorporates the existence of an underlying lattice. As mentioned above, the lattice seems to play a crucial role to sustain a turbulent regime. Such a nonadiabatic effect would be indeed interesting to understand.

ACKNOWLEDGMENTS

The authors acknowledge J. Lega, H. Chaté, P. Manneville, B. Shraiman, E. Siggia, V. Croquette, Y. Couder, M. Rabaud, S. Michalland, A. Pumir, M. Dubois, P. Bergé, and F. Daviaud, for enlightening discussions, and G. Bouzerar for his participation in this work. This work has been supported by CNRS, DRET, Ecole Normale Superieure, and Universities Paris VI and Paris VII.

[1] H. Chaté and P. Manneville, Phys. Rev. Lett. **58**, 112 (1987); see also a precursor paper by K. Kaneko, Prog. Theor. Phys. **74**, 1033 (1985).

[2] S. Ciliberto and P. Bigazzi, Phys. Rev. Lett. **60**, 286 (1988); F. Daviaud, M. Dubois, and P. Bergé, Europhys. Lett. **9**, 441 (1989); M. Rabaud, S. Michalland, and Y. Couder, Phys. Rev. Lett. **64**, 184 (1990); see also A. Erzan and S. Sinha, *ibid.* **66**, 2750 (1991).

[3] Such an analogy was suggested by Y. Pomeau; see P. Manneville, in *Dissipative Structure and Weak Turbulence,* edited by Araki, Libchaber, and Parisi (Academic, Boston, 1991).

[4] F. Daviaud, M. Bonetti, and M. Dubois, Phys. Rev. A **42**, 3388 (1990).

[5] F. Daviaud, J. Lega, P. Bergé, P. Coullet, and M. Dubois, Physica D **55**, 287 (1992). Spatiotemporal intermittency in complex Ginsburg-Landau equations has recently been obtained by H. Chaté (private communication).

[6] N. Bekki and K. Nozaki, Phys. Lett. **110A**, 133 (1985); J. Lega, B. Janiaud, S. Jucquois, and V. Croquette, Phys. Rev. A **45**, 5596 (1992).

[7] O. Cardoso, H. Willaime, and P. Tabeling, Phys. Rev. Lett. **65**, 1869 (1990); H. Willaime, O. Cardoso, and P. Tabeling, *ibid.* **67**, 3247 (1991).

[8] H. Willaime, O. Cardoso, and P. Tabeling, Eur. J. Mech., B/Fluids, Suppl. II **10**, 165 (1991).

[9] P. Tabeling, B. Perrin, and S. Fauve, Europhys. Lett. **3**, 459 (1987); P. Tabeling, O. Cardoso, and B. Perrin, J. Fluid Mech. **213**, 511 (1990).

[10] See, for instance, S. Rasenat, G. Hartung, B. L. Winkler, and I. Rehberg, Exp. Fluids **7**, 412 (1989).

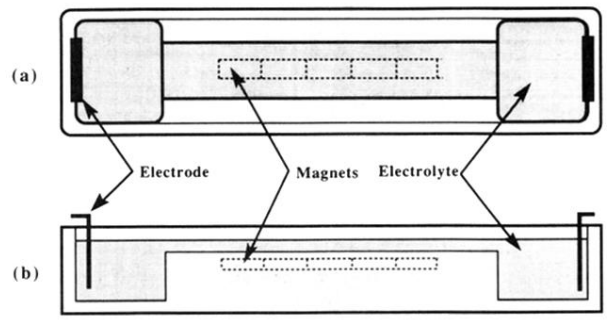

FIG. 1. Sketch of the experiment, with (a) and (b) the top and side views, respectively. The light gray region corresponds to the fluid, and the dark gray to the electrodes.

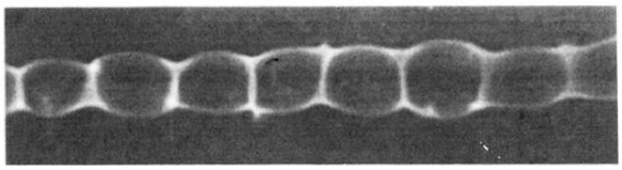

FIG. 4. Shadowgraph image of a system of 15 corotating vortices, produced by 30 magnets, with a fluid thickness of 3 mm.